PHYSICAL REVIEW D **90,** 045038 (2014)

Validating the 2PI resummation: The Bloch-Nordsieck example

A. Jakovác[*]
Institute of Physics, Eötvös University, H-1117 Budapest, Hungary

P. Mati[†]
Institute of Physics, Budapest University of Technology and Economics, H-1111 Budapest, Hungary;
Institute of Physics, Eötvös University, H-1117 Budapest, Hungary;
and MTA-DE Particle Physics Research Group, University of Debrecen,
P.O. Box 105, H-4010 Debrecen, Hungary
(Received 26 May 2014; published 27 August 2014)

In this work, we provide a numerical method to obtain the Bloch–Nordsieck spectral function at finite temperature in the framework of the 2-particle-irreducible (2PI) approximation. We find that the 2PI results nicely agree with the exact one, provided we perform a coupling constant matching. In the paper, we present the resulting finite temperature running of the 2PI coupling constant. This result may apply for the finite temperature behavior of the coupling constant in QED, too.

DOI: 10.1103/PhysRevD.90.045038 PACS numbers: 11.15.-q, 11.10.Gh, 11.10.Wx, 12.20.-m

I. INTRODUCTION

The infrared limit of the QED was modeled by Bloch and Nordsieck in 1937, and their treatment of the IR singularities has become a textbook material since. In the framework of the Bloch–Nordsieck (B-N) model, one is able to resum all of the radiative contributions to the fermionic Green's function generated by ultrasoft photons. A detailed discussion of this calculation can be found in the original paper of Bloch and Nordsieck [1], in Refs. [2] and [3], and in Ref. [4].

The relevance of this model is twofold. On the one hand, it is an exactly solvable gauge theory, and in this respect it plays a unique role. On the other hand, the model is designed to describe the real QED in the deep IR limit, and so this is capable to give a hint about how one has to treat the IR divergences of gauge theories. In particular, it can be used to prove IR theorems in QED [5].

Besides an exact solution, one can also give solutions in different approximations. In particular the 2-particle-irreducible (2PI) approximation [6] is a well-known tool to study the quasiparticle properties of the system. One of the biggest challenge in front of the 2PI techniques is the representations of symmetries: although the 2PI technique is capable of realizing all global symmetries [6,7], it is only at the level of the effective action and not in the computations. In particular, the treatment of local gauge symmetries is rather tedious [8,9]. The study of the B-N model provides an excellent tool to test the reliability of fixed gauge calculations.

In Ref. [4], we used the 2PI functional method to study the B-N model at zero temperature. The spectrum could be obtained by applying numerical calculations. We found on the one hand the disappointing fact that the fit comparison to the exact propagator was not very promising (see Ref. [4]); on the other hand, unlike in the old-fashioned perturbation theory, the spectrum remained regular even in the highly IR regime (no IR singularity observed at the mass shell). We remark that also in other physical situations one can observe that one needs resummation beyond the 2PI level [10]. The role of multiple scattering is emphasized also in Ref. [11].

At finite temperature there are several studies in the literature [12–14] to derive the behavior of the fermion propagator. In our paper [4], we developed a method to reproduce the exact result using the Ward–Takahashi identities at zero temperature (cf. also Ref. [15]). This could have been generalized to finite temperature in Ref. [16]. With the help of this method, we managed to obtain a fully analytic form of the excitation spectrum. Having these analytic results gives us a perfect opportunity to investigate the validity of the 2PI quasiparticle description of an interacting quantum field theory at finite temperature.

The purpose of the present paper is to show how the 2PI works at finite temperature. We will derive the spectral function numerically and compare it to the exactly calculated case. The upshot is there exists a mapping between the coupling constants of the 2PI and the exact results in such a way that the two spectral functions overlap almost entirely. This is a highly nontrivial result, since the exact spectral function is an asymmetric function of the frequency, rather different from a simple Lorentzian. The most important message to the 2PI community is that our result validates the 2PI approximation method at nonzero temperature, and only a finite reparametrization of the theory is needed.

From the perturbative point of view, the 2PI technique resums the 2PI diagrams, but the coupling constant and also the higher point functions are remained unchanged. So for a

[*]jakovac@caesar.elte.hu
[†]mati@phy.bme.hu; matipeti@gmail.com

certain 2PI diagram, there exists another infinite set of diagrams providing coupling constant modification. In the sense of the renormalization group, we may try to take into account the sum of these diagrams effectively as a temperature-dependent (running) coupling constant. Since we now know the value of an observable exactly (the electron spectral function for any frequency and temperature in a given gauge), the best method to extract the temperature-dependent coupling is to compare the 2PI and the exact results. This is done in the present paper.

The structure of the paper is as follows. First, we give an introduction to the B-N model itself and to the conventions of the finite temperature real time formalism. In Sec. III, we recap the zero-temperature results: the one-loop correction obtained from perturbation theory (PT) and the implementation of the 2PI numerics. In Sec. IV, we derive the one-loop self-energy at $T \neq 0$ and show its consistency with the zero-temperature result by taking the $T \to 0$ limit. Then, we calculate the expression for the discontinuity of the self-energy for the 2PI procedure. The numerical implementation of the calculation happens in a similar fashion as the zero temperature one. In Sec. V, we present our results obtained from the numerics and the comparison to the exact result [16]. We found a nontrivial mapping of the coupling between the two calculation methods from which we conclude the following: the 2PI, although it is an approximation, at finite temperature gives a perfect qualitative description of the collective excitation of the system.

II. PROPERTIES OF THE BLOCH–NORDSIECK MODEL

The B-N model was designed to describe accurately the low-energy regime of quantum electrodynamics. Considering the contributions to the fermion self-energy only from the deep IR photons, reducing the Dirac spinor to a one-component fermion is well justified. Indeed, at this energy scale, photons do not have enough energy even to flip the spin of the fermion, not to mention the pair creation [1]. In this respect, one can substitute a 4-vector u_μ in the place of the γ_μ matrices, which is considered as the 4-velocity of the fermion.

The Lagrangian then reads

$$\mathcal{L} = -\frac{1}{4} F_{\mu\nu} F^{\mu\nu} + \Psi^\dagger (i u_\mu D^\mu - m)\Psi, \tag{1}$$

where the usual notations for the field-strength tensor and for the covariant derivative are used: $F_{\mu\nu} = \partial_\mu A_\nu - \partial_\nu A_\mu$ and $D_\mu = i\partial_\mu - eA_\mu$, respectively. Later, we will also use the standard notation $\alpha = e^2/(4\pi)$. In the above formula, u_μ is a 4-velocity, but we can also choose the form $u = (1, \mathbf{v})$, with $\mathbf{v} = \mathbf{u}/u_0$ by rescaling the fermionic field as $\Psi \to \Psi/\sqrt{u_0}$ and the fermion mass by $m \to m u_0$.

It is possible to obtain exactly the full fermion propagator associated with this theory both for zero and finite temperatures as it is presented in Refs. [4] and [16], respectively. Now, we are going to discuss the notations and conventions that we are using in this paper.

For the calculations, we use the real-time formalism (details are in Refs. [16] and [17]). The propagators are matrices in this convention,

$$\begin{aligned} i\mathcal{G}_{ab}(x) &= \langle T_C \Psi_a(x) \Psi_b^\dagger(0)\rangle \quad \text{and} \\ iG_{\mu\nu,ab}(x) &= \langle T_C A_{\mu a}(x) A_{\nu b}(0)\rangle, \end{aligned} \tag{2}$$

where T_C denotes ordering with respect to the contour variable (contour time ordering). At finite temperature with help of the Kubo-Martin-Schwinger relation, we can determine G_{12} and G_{21},

$$\begin{aligned} iG_{12}(k) &= \pm n_\pm(k_0)\varrho(k), \\ iG_{21}(k) &= (1 \pm n_\pm(k_0))\varrho(k), \end{aligned} \tag{3}$$

where

$$n_\pm(k_0) = \frac{1}{e^{\beta k_0} \mp 1} \quad \text{and} \quad \varrho(k) = iG_{21}(k) - iG_{12}(k) \tag{4}$$

are the distribution functions [Bose–Einstein (+) and Fermi–Dirac (−) statistics] and the spectral function, respectively, while $\beta = 1/T$ is the inverse temperature. We will also use R/A formalism [16], where

$$G_{rr} = \frac{G_{21} + G_{12}}{2}, \qquad G_{ra} = G_{11} - G_{12}, \qquad \varrho = iG_{ra} - iG_{ar}. \tag{5}$$

The G_{ra} propagator is the retarded, the G_{ar} is the advanced propagator, and G_{rr} is usually called the Keldysh propagator.

At zero temperature, the (free) fermionic Feynman propagator reads

$$\mathcal{G}_0(p) = \frac{1}{u_\mu p^\mu - m + i\varepsilon}. \tag{6}$$

It has a single pole, which means that there are no antiparticles in the model. Consequently, closed fermion loops are excluded, and thus there is no self-energy correction to the photon propagator at zero temperature. Physically, this means that the energy is not sufficient to excite the antiparticles. We interpret u^μ as the fermionic 4-velocity, and since it is fixed, the soft photons cannot change it (no fermion recoil). In fact, this means that the fermion is a hard probe of the system and hence not part of the thermal medium [12,13]. This is also supported by the spin-statistics theorem [18], which would forbid a one-component fermion field. Consequently, we will neglect the "12" fermion propagator, too: $\mathcal{G}_{12} = 0$.

The exact photon propagator reads in the Feynman gauge

$$G_{ab,\mu\nu}(k) = -g_{\mu\nu}G_{ab}(k), \qquad G_{ra} = \frac{1}{k^2}\bigg|_{k_0\to k_0+i\varepsilon},$$
$$\varrho(k) = 2\pi \mathrm{sgn}(k_0)\delta(k^2), \tag{7}$$

and all other propagators can be expressed using identities (3) and (5).

III. RECAP OF T = 0 2PI CALCULATIONS

The main idea is to use the exact propagators in the perturbation theory as building blocks of a loop integral, where the exact propagator is determined self-consistently using skeleton diagrams as resummation patterns. The one-loop 2PI fermion self-energy diagram in the case of the B-N model generates the resummation of all the "rainbow" diagrams. One needs to take care of the UV divergences, too, on which we perform a renormalization with the same form of divergent parts of the counterterms as in the one-loop case.

At zero temperature, we have the following self-consistent system of equations in the 2PI approximation:

$$\mathcal{G}(p) = \frac{1}{\mathcal{G}_0^{-1}(p) - \Sigma(p)}, \tag{8}$$

$$-i\Sigma(p) = (-ie)^2 \int \frac{d^4k}{(2\pi)^4} iG_{\mu\nu}(k) i\mathcal{G}(p-k). \tag{9}$$

Here, $\mathcal{G}_0$ and $\mathcal{G}$ stand for the free and the dressed fermion propagator. $G_{\mu\nu}$ is the photon propagator.

A. One-loop correction

In strict PT we use the propagators from Eqs. (6) and (7) to compute the self-energy. We choose a reference frame in which $u^\mu = (1,0,0,0)$, and we find using dimensional regularization

$$\Sigma_{1\mathrm{loop}}(p_0) = \frac{\alpha}{\pi}(p_0 - m)\left(-\ln\frac{m-p_0}{\mu} + \mathcal{D}_\epsilon\right). \tag{10}$$

Here, μ is the renormalization scale. The divergent part $\mathcal{D}_\epsilon$ has the following expression:

$$\mathcal{D}_\epsilon = \frac{1}{2\epsilon} + \frac{1}{2}(\ln 4\pi - \gamma_E). \tag{11}$$

We renormalized the self-energy using the $\overline{\mathrm{MS}}$ scheme, by which the counterterms read as

$$\delta Z_{1,\overline{\mathrm{MS}}} = \delta_{m,\overline{\mathrm{MS}}} = \frac{\alpha}{\pi} D_\epsilon, \tag{12}$$

where $\delta Z_{1,\overline{\mathrm{MS}}}$ and $\delta_{m,\overline{\mathrm{MS}}}$ are the wave function renormalization and the multiplicative mass renormalization, respectively. Hence, the renormalized self-energy is

$$\Sigma^{\mathrm{ren}}_{1\mathrm{loop}} = -\frac{\alpha}{\pi}(p_0 - m)\ln\frac{m-p_0}{\mu}. \tag{13}$$

For details, see Ref. [4].

B. 2PI procedure at $T = 0$

In the 2PI approach, we treat Eqs. (8) and (9) self-consistently. Then, we implement the following steps numerically [4], which will be applied at finite T, too:

(i) Step 1: We calculate the discontinuity of the self-energy in order to use it for the spectral representation of the retarded Green's function. In the B-N model, due to the missing antiparticles, the retarded and the Feynman propagators are the same, and so we can work with the simpler Feynman propagators. Later, at finite temperature, this procedure will be used for the retarded Green's function (cf. Sec. IV):

$$\Sigma(p) = ie^2 \int \frac{d^4k}{(2\pi)^4} G_{\mu\nu}\mathcal{G}(p-k)$$
$$= ie^2 \int_0^\infty \frac{d\omega}{2\pi}\int \frac{d^4k}{(2\pi)^4}\frac{1}{k^2+i\epsilon}\frac{\rho(\omega)}{p_0 - k_0 - \omega + i\epsilon} \tag{14}$$

$$\Sigma(p) = \int_0^\infty \frac{d\omega}{2\pi}\rho(\omega)\Sigma_{1-\mathrm{loop}}(p,\omega). \tag{15}$$

Now, we can take the discontinuity

$$\underset{p_0}{\mathrm{Disc}}\Sigma(p) = \int_0^\infty \frac{d\omega}{2\pi}\rho(\omega)\underset{p_0}{\mathrm{Disc}}\Sigma_{1-\mathrm{loop}}(p,\omega)$$
$$= \frac{\alpha}{\pi}\int_0^\infty d\omega(p_0-\omega)\rho(\omega). \tag{16}$$

In both equations, we introduced the fermion spectral function $\rho(p)$. In our algorithm, it serves as an input, which is usually the free fermion spectral function $\rho(p) = 2\pi\delta(p-m)$.

(ii) Step 2: Here, we calculate the real part of self-energy from its discontinuity. For this purpose, we use the Kramers–Kronig relation:

$$\mathrm{Re}\Sigma(p_0,\mathbf{p}) = \int_{-\infty}^{\infty} \frac{d\omega}{2\pi} \frac{\mathrm{Disc}_\omega i\Sigma(\omega,\mathbf{p})}{p_0-\omega+i\epsilon}. \quad (17)$$

(iii) Step 3: We renormalize the real part of the self-energy using the "on-mass-shell" renormalization scheme:

$$\mathrm{Re}\Sigma(p_0=m)=0, \quad (18)$$

$$\left.\frac{d\mathrm{Re}\Sigma(p_0)}{dp_0}\right|_{p_0=m}=0. \quad (19)$$

(20)

(iv) Step 4: From all of this information, we construct the new spectral function, which reads as

$$\rho(p) = \frac{2\mathrm{Im}\Sigma(p)}{(p_0-m-\mathrm{Re}\Sigma(p))^2+(\mathrm{Im}\Sigma(p))^2}. \quad (21)$$

(v) Step 5: We set the new spectral function to be our new input and iterate this procedure until it converges.

(vi) Step 4+: As an additional step, we had to include a rescaling of the spectral function, which was necessary to stabilize the convergence. This step is not needed at nonzero temperature.

For the zero-temperature case, we obtained the dressed propagator for the fermion. From the analysis, it turned out that this result, being an approximation, is far from the exact solution, although it is IR finite, which cannot be claimed about the PT calculation (see Ref. [4]).

IV. NONZERO TEMPERATURE

We are working in the real-time formalism; hence, the Green's functions in this picture are going to have a matrix structure. We choose the R/A basis for the matrix representation to calculate the retarded self-energy. First, we are going to consider the one-loop correction, and then we present a derivation of the 2PI resummed spectral function at finite temperature. To evaluate its self-consistent equations, we will use a numerical approach that is similar to what we discussed above for the $T=0$ case.

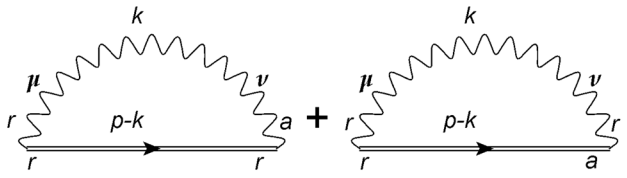

FIG. 1. The diagrammatic representation of the self-energy. The wavy line corresponds to the free (here also the exact) photon propagator with a loop momentum k, and the double solid line is for the exact fermion propagator with momentum $p-k$. Both the polarization and the Keldysh indices are shown.

The integral equation for the retarded self-energy at nonzero temperature in the Feynman gauge reads as

$$\Sigma_{ar}(p) = ie^2\int \frac{d^4k}{(2\pi)^4}[G_{rr}(k)\mathcal{G}_{ra}(p-k)+G_{ra}(k)\mathcal{G}_{rr}(p-k)], \quad (22)$$

where G and $\mathcal{G}$ stand for the propagator of the photon and the fermion, respectively. In Fig. 1, we can see the pictorial representation of the fermion self-energy using Feynman diagrams.

Now, if we take the discontinuity, we will have

$$\underset{p_0}{\mathrm{Disc}}\Sigma_{ar}(p) = e^2\int\frac{d^4k}{(2\pi)^4}[G_{rr}(k)\rho_f(p-k)+\rho_\gamma(k)\mathcal{G}_{rr}(p-k)]. \quad (23)$$

Here, ρ_f and ρ_γ are the spectral functions to the fermion and the photon, respectively. In general, we can express the rr propagators by the spectral function combining with the Bose–Einstein or Fermi–Dirac distributions, respectively:

$$\mathcal{G}_{rr}(p) = \left(\frac{1}{2}-n_-(p_0)\right)\rho_f(p), \quad (24)$$

$$G_{rr}(p) = \left(\frac{1}{2}+n_+(p_0)\right)\rho_\gamma(p). \quad (25)$$

When inserting these expressions into Eq. (23), we get

$$\begin{aligned}\underset{p_0}{\mathrm{Disc}}\Sigma_{ar}(p) &= e^2\int\frac{d^4k}{(2\pi)^4}\left[\left(\frac{1}{2}+n_+(k_0)\right)\rho_\gamma(k)\rho_f(p-k)+\rho_\gamma(k)\left(\frac{1}{2}-n_-(p_0-k_0)\right)\rho_f(p-k)\right]\\ &= e^2\int\frac{d^4k}{(2\pi)^4}(1+n_+(k_0)-n_-(p_0-k_0))\rho_\gamma(k)\rho_f(p-k). \end{aligned} \quad (26)$$

In the last step of Eq. (26), we get the most general form of the equation, as long as we do not specify the corresponding spectral functions.

A. One-loop correction at $T \neq 0$

For the one-loop case, we have to plug in the spectral function of the free theory both for the fermion and gauge fields. By performing this substitution, our equation reads as

$$\begin{aligned}\underset{p_0}{\mathrm{Disc}}\Sigma_{ar}(p) &= e^2\int\frac{d^4k}{(2\pi)^4}(1+n_+(k_0)-n_-(p_0-k_0))2\pi\mathrm{sgn}k_0\delta(k_0^2-\mathbf{k}^2)2\pi\delta(u_0(p_0-k_0)-\mathbf{u}(\mathbf{p}-\mathbf{k})-m)\\ &= \frac{e^2}{8\pi^3}\int_0^\infty dk\mathbf{k}^2\int_{-1}^{1}dx\frac{(2\pi)^2}{2|\mathbf{k}|}[(1+n_+(|\mathbf{k}|)-n_-(p_0-|\mathbf{k}|))\delta(u_0p_0-\mathbf{up}-u_0|\mathbf{k}|-|\mathbf{u}||\mathbf{k}|x-m)\\ &\quad+(n_+(|\mathbf{k}|)+n_-(p_0+|\mathbf{k}|))\delta(u_0p_0-\mathbf{up}+u_0|\mathbf{k}|-|\mathbf{u}||\mathbf{k}|x-m)].\end{aligned}\tag{27}$$

Here, we introduced the variable x, which stands for the cosine of the angle between the two spatial 3-vectors $\mathbf{u}$ and $\mathbf{k}$. For the sake of simplicity, in the following, we are going to use the notations $pu \equiv p_0u_0 - \mathbf{pu}$ for the Minkowski product, and $k \equiv |\mathbf{k}|$, $u \equiv |\mathbf{u}|$ for the absolute values of the 3-vectors $\mathbf{k}$ and $\mathbf{u}$, respectively.

First, we perform the angular integration for x:

$$\underset{p_0}{\mathrm{Disc}}\Sigma_{ar}(p) = \frac{e^2}{4\pi u}\left(\Theta(pu-m)\int_{\frac{pu-m}{u+u_0}}^{\frac{pu-m}{u-u_0}}dk(1+n_+(k)-n_-(p_0-k))+\Theta(m-pu)\int_{\frac{m-pu}{u+u_0}}^{\frac{m-pu}{u-u_0}}dk(n_+(k)+n_-(p_0+k))\right).\tag{28}$$

Now, we are going to use the fact that the fermion in this system is a hard probe, and thus it is not part of the heat bath [12,13]. This manifests already in Eq. (26) in a way that we need to set the Fermi–Dirac distribution to zero; otherwise, we would face inconsistencies when trying to take the $T \to 0$ limit:

$$n_f \equiv 0 \quad \text{(in the B-N framework)}.\tag{29}$$

In that case, Eq. (28) simplifies in the following way:

$$\underset{p_0}{\mathrm{Disc}}\Sigma_{ar}(p) = \frac{e^2}{4\pi u}\int_{\frac{pu-m}{u+u_0}}^{\frac{pu-m}{u-u_0}}dk(1+n_+(k)).\tag{30}$$

Evaluating the integral, we get a result consistent with the $T = 0$ case:

$$\begin{aligned}\underset{p_0}{\mathrm{Disc}}\Sigma_{ar}(p) &= \frac{e^2}{2\pi}\Theta(pu-m)(pu-m)\\ &\quad+\frac{Te^2}{4\pi u}\ln\left(\frac{1-e^{-\beta\frac{pu-m}{u-u_0}}}{1-e^{-\beta\frac{pu-m}{u+u_0}}}\right).\end{aligned}\tag{31}$$

This gives us the desired result for the $T \to 0$ limit, namely, $\underset{p_0}{\mathrm{Disc}}\Sigma_{ar}(p) = \frac{e^2}{2\pi}\Theta(pu-m)(pu-m)$.

B. Nonzero temperature calculations for the 2PI scheme

Now, we are going to derive the 2PI resummed result for the finite-temperature theory. Let us consider Eqs. (8) and (22). Instead of calculating the one-loop correction by inserting free propagators, we are going to use the self-consistent fermion propagator so defining a self-consistent system of integral equations. We stick to the physical picture that the fermion is not part of the thermal medium, Eq. (29). Using the calculation in Eq. (27), we arrive at an expression for the discontinuity of the self-energy for the general fermion propagator:

$$\begin{aligned}\underset{p_0}{\mathrm{Disc}}\Sigma_{ar}(p) &= e^2\int\frac{d^4k}{(2\pi)^4}(1+n_b(k_0))\rho_\gamma(k)\rho_f(p-k)\\ &= e^2\int\frac{d^4k}{(2\pi)^4}(1+n_b(k_0))\\ &\quad\times\frac{2\pi}{2k}(\delta(k_0-k)-\delta(k_0+k))\bar{\rho}_f(up-uk-m).\end{aligned}\tag{32}$$

Here, we used the free photon propagator as above, and for the general spectral function of the fermion, we introduced the notation $\rho_f(p) = \bar{\rho}_f(up-m)$. After some algebra, we find

$$\underset{p_0}{\mathrm{Disc}}\Sigma_{ar}(p) = \frac{e^2}{8\pi^2}\int_{-\infty}^{\infty}dk\int_{-1}^{1}dxkn_b(k)\bar{\rho}_f(w+(u_0+ux)k).\tag{33}$$

Here, we defined $w := up - m$, and x represents the angle between the spatial parts of k^μ and u^μ, so xku is the scalar product of two three-dimensional vectors like in the one-loop calculation. Actually, this can be written in a more elegant and, for the numerical implementation, a more useful way. We introduce the variable z as the argument of the function $\bar{\rho}_f$:

$$\underset{p_0}{\mathrm{Disc}}\Sigma_{ar}(p) = \frac{e^2}{8\pi^2}\frac{1}{u}\int_{-\infty}^{\infty} dk \int_{w+(u_0-u)k}^{w+(u_0+u)k} dz\bar{\rho}_f(z)n_b(k)$$
$$= \frac{e^2}{8\pi^2}\frac{1}{u}\int_{-\infty}^{\infty} dz\bar{\rho}_f(z)\int_{\frac{z-w}{u_0-u}}^{\frac{z-w}{u_0+u}} dk n_b(k). \quad (34)$$

In the case in which the length of the 3-velocity tends to zero, $u \to 0$, we have

$$\underset{p_0}{\mathrm{Disc}}\Sigma_{ar}(p_0) = \frac{\alpha}{\pi}\int_{-\infty}^{\infty} dz\bar{\rho}_f(z)(p_0 - m - z) \times (1 + n_b(p_0 - m - z)). \quad (35)$$

For $u \neq 0$,

$$\underset{p0}{\mathrm{Disc}}\Sigma_{ar}(w) = \frac{\alpha}{2\pi}\int_{-\infty}^{\infty} dz\bar{\rho}_f(z)\frac{T}{u}\ln\frac{1 - e^{-\beta\frac{z-w}{u_0-u}}}{1 - e^{-\beta\frac{z-w}{u_0+u}}}. \quad (36)$$

We set $m = 0$, and this can be done without the loss of generality since the two expressions in Eqs. (35) and (36) depend on the variable $w = up - m$ only. That means the theory is not sensitive where the mass-shell is placed; it can be anywhere on the real line.

V. 2PI RESULTS

We are implementing the same numerical method that we used for the zero-temperature case (step 1–step 5 in Sec. III B), using the finite-temperature form of Eq. (16), which is given in Eqs. (35) and (36). In the numerical procedure, we fix the value of the coupling and the numerical value of the temperature and perform the iteration until it converges. The physical temperature is a dimensionful quantity; therefore, dimensionless quantities must depend only on the temperature only through the other dimensionful parameter. If there were no renormalization problem, then the only quantity, which can make temperature dimensionless, would be w, and the results would depend on βw. However, renormalization leads to the appearance of a quantum scale through dimensional transmutation (for the B-N model; see Ref. [4]). This can be characterized, for example, by the value of the Landau pole Λ_{BN}; then, the results will implicitly depend on $\beta\Lambda_{BN}$. In the numerics, it shows up as a dependence of the physical results not only on βw but also separately on the numerical value of the temperature. We will refer this numerical value as "dimensionless temperature," knowing that only ratios of these dimensionless temperature values have physical meaning.

The result of the iteration is the spectral function. First, we observe that a small thermal mass Δm_T is generated, in dimensionless units in the order of $\Delta m_T/T \sim 10^{-3}$. Interestingly, this thermal mass is negative; it shifts the spectral function to the left. In the exact solution in Ref. [16], we found a zero thermal mass, and thus we can consider it as an artifact of the 2PI approximation, which can be incorporated into the mass and finally into $w = up - m - \Delta m_T$.

A. Zero-velocity case

By applying the algorithm described in Sec. III. B, we can obtain the spectral function derived from the 2PI approximation for the theory, using Eq. (35) as the self-energy input. In Fig. 2, we can see the spectral function for

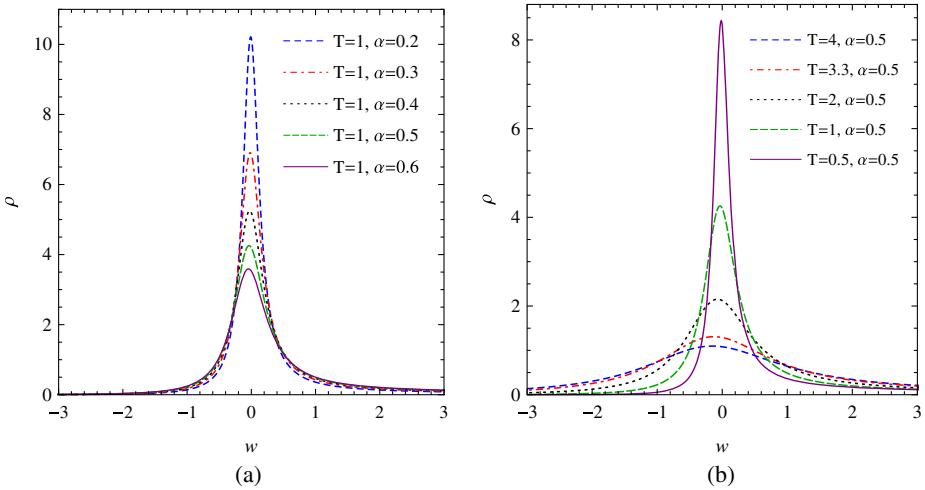

FIG. 2 (color online). The coupling constant dependence of the spectral function in the 2PI approximation (a) at fixed temperature $T = 1$ and (b) at a fixed coupling value, $\alpha = 0.5$. The curves widen with growing coupling and growing temperature.

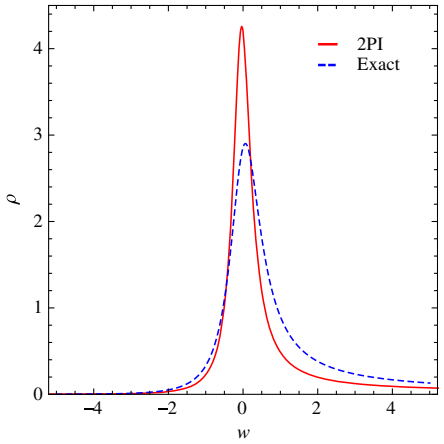

FIG. 3 (color online). Comparing the 2PI resummed spectral function to the exact one. The solid red line is obtained from the 2PI resummation, while the dashed blue line is the exact spectral function. Both of them are at $T = 1$, and the couplings are $\alpha_{ex} = \alpha_{2PI} = 0.5$.

different coupling values and for different temperatures. The spectrum exhibits a pole, and its width is growing with increasing coupling constant and with increasing temperature.

In the Dyson–Schwinger approach, the exact spectral function can be derived in a closed form (at least in the zero-velocity case). We wish to compare the 2PI results to our analytic expression obtained in Ref. [16]:

$$\rho(w) = \frac{N_\alpha \beta \sin(\alpha) e^{\beta w/2}}{\cosh(\beta w) - \cos(\alpha)} \frac{1}{|\Gamma(1 + \frac{\alpha}{2\pi} + i\frac{\beta w}{2\pi})|^2}. \quad (37)$$

Here, we use the notation $w = p_0 - m$ again, and N_α is a normalization factor. Both for the 2PI approximation and the Dyson–Schwinger calculation, we assumed a normalization prescription, which assigned by the $\int_w \rho = 1$ sum rule.

To check the quality of the 2PI approximation, we can compare the resulting spectral function with the exact one. The comparison can be seen on Fig. 3. We can see immediately that the two spectra are not very similar. The reason is, as we discussed in the introduction, that the 2PI approximation does not sum up all the diagrams, in particular, the coupling constant corrections. To improve the 2PI calculation, therefore, we can try to take into account the resummation of these diagrams effectively in a renormalization-group-inspired way, as a temperature-dependent coupling constant. We should use a non-perturbative matching procedure and choose a value of α_{2PI} that reproduces the exact result the most accurately. For a perfect matching, not only the coupling constant but also the higher point functions should also be resummed. But we may hope that the most important effect comes from the relevant couplings, in this case from α_{2PI}.

Therefore, our strategy will be to find the best, temperature-dependent value of the coupling constant α_{2PI} that yields the best match between the exact and the 2PI spectral functions. As we can see in Fig. 4, there exists such a value, for which the matching is almost perfect. We can observe that the fit is excellent not just at the close vicinity of the peak region but also for a much larger momentum regime, and it can give an account also for the asymmetric form of the exact spectral function. For asymptotically large momenta, we expect that the two curves do not agree, according to Ref. [4], and this can also be observed in Fig. 4. This result is a strong argument in favor of the usability of the 2PI technique at finite temperature also for gauge theories.

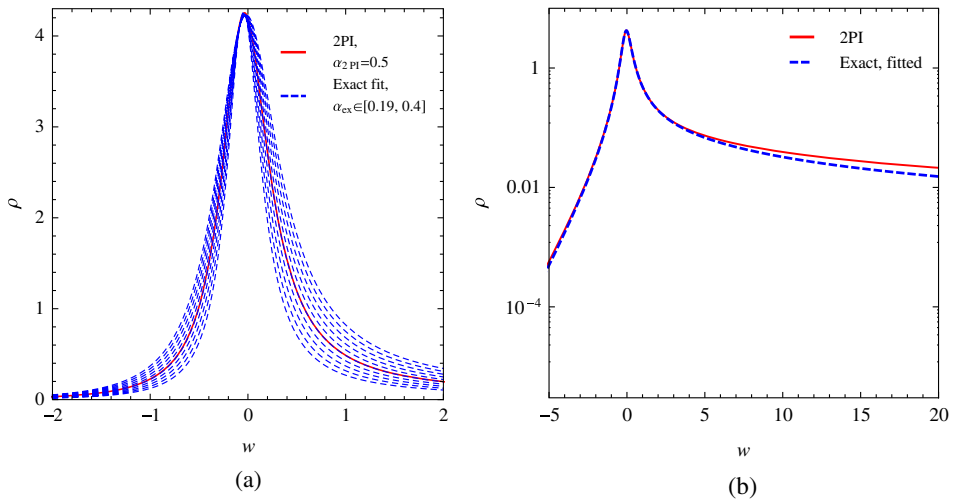

FIG. 4 (color online). The fitting of the exact spectral function on the 2PI spectrum on (a) linear and (b) logarithmic plots. On the plot, the curves are normalized to the same height for better visibility. We can see an exact match at the peak and a small deviation in the asymptotics. The fit yields $\alpha_{2PI} = 0.5$ for $\alpha_{ex} = 0.293$ at $T = 1$.

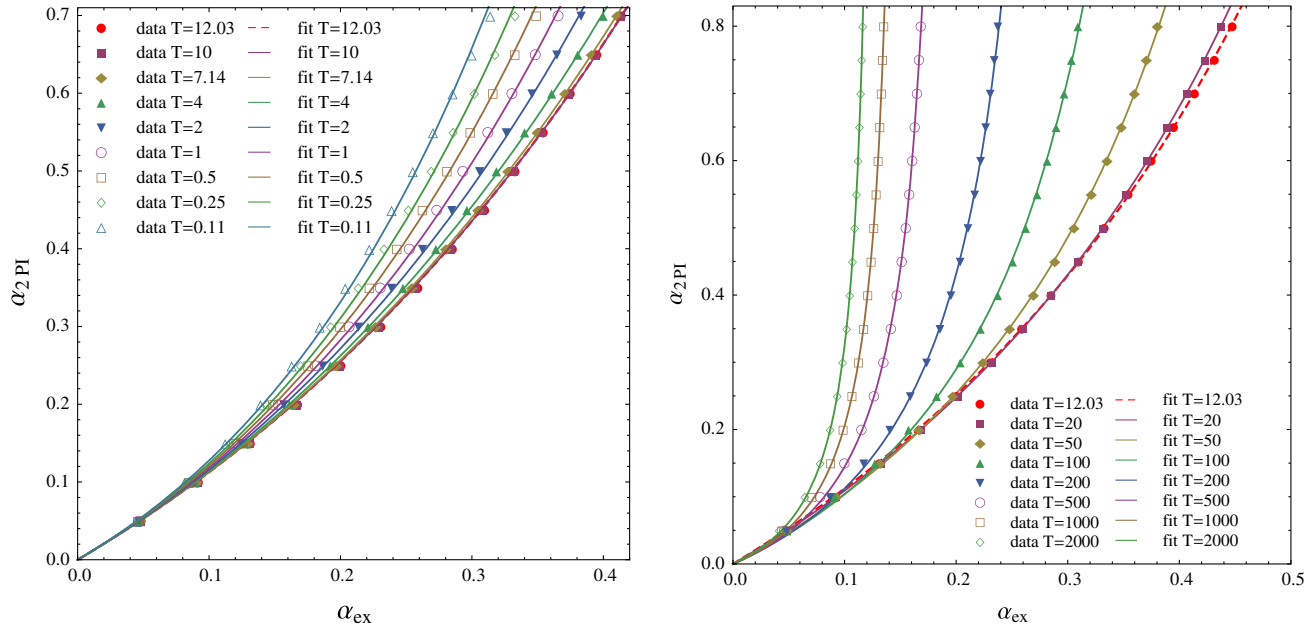

FIG. 5 (color online). The relation between the 2PI and the exact coupling at $u = 0$ for temperatures (a) $T \in [0, 12.03]$ and (b) $T \in (12.03, \infty)$, respectively. The dashed red line indicates the limiting function at $T = 12.03$; for details, see the text.

Hence, we can say that the coupling, which takes the value of $\alpha_{2\mathrm{PI}} = 0.5$ in the 2PI resummation at $T = 1$, is equivalent to $\alpha_{\mathrm{ex}} = 0.293$ in the Dyson–Schwinger calculation at the same temperature. One can also conclude that the vertex corrections (which are absent in the 2PI self-energy calculations) have a role to modify the value of the renormalized coupling. In the following, we are going to look for a general relation between $\alpha_{2\mathrm{PI}}$ and α_{ex}.

We can repeat the strategy above for different temperatures. In this way, we can determine a relation $\alpha_{2\mathrm{PI}}(\alpha_{\mathrm{ex}}, T)$ [technically, it is simpler to obtain $\alpha_{\mathrm{ex}}(\alpha_{2\mathrm{PI}}, T)$ and invert this relation]. This provides the finite-temperature dependence, or finite-temperature "running," of the 2PI coupling constant.

We expect that for small couplings the exact and the perturbative values agree, since the perturbation theory gives $\alpha_{\mathrm{ex}} = \alpha_{2\mathrm{PI}} + \mathcal{O}(\alpha_{2\mathrm{PI}}^2)$. This is indeed the case. For larger couplings, however, the linear relation changes. Interestingly, we can observe that two different types of functions describe the relation between the couplings depending on the temperature. The first type of function, which gives the mapping between the two couplings, is valid in the interval $T \in [0, 12.03]$. This relation can be obtained by a one-parameter fit between the 2PI and the exact couplings, namely,

$$\alpha_{2\mathrm{PI}} = A_T(e^{\frac{\alpha_{\mathrm{ex}}}{A_T}} - 1). \tag{38}$$

The result is shown in Fig. 5(a), and the fit parameters (A_T) are listed in Tables I and II. From this relation, we immediately see that for small $\alpha_{2\mathrm{PI}}$ the relation of the couplings is linear:

$$\alpha_{2\mathrm{PI}} \approx \alpha_{\mathrm{ex}} + \mathcal{O}\left(\frac{\alpha_{\mathrm{ex}}^2}{A_T}\right). \tag{39}$$

TABLE I. The fit parameters in the low-temperature case. The error of the parameters is ± 0.001.

T	0.11	0.25	0.5	1	2	4	7.14	10	12.03
A_T	0.213	0.242	0.27	0.305	0.343	0.384	0.414	0.426	0.429

TABLE II. The fit parameters in the high-temperature case.

T	20	50	100	200	500	1000	2000
B_T	1.03 ± 0.003	1.118 ± 0.008	1.217 ± 0.014	1.312 ± 0.017	1.381 ± 0.016	1.38 ± 0.012	1.3 ± 0.006
C_T	1.107 ± 0.001	1.668 ± 0.025	2.654 ± 0.054	4.241 ± 0.083	6.937 ± 0.105	8.951 ± 0.1	9.991 ± 0.055

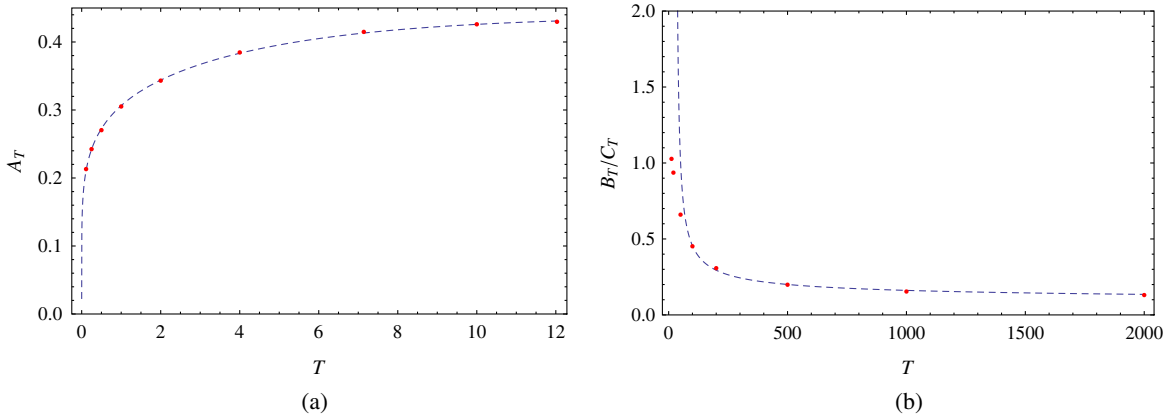

FIG. 6 (color online). The running of (a) A_T and (b) B_T/C_T with respect to the temperature. This latter quantity is the position of the pole [cf. Eq. (42)]. One can see the best matching on higher temperatures.

This tells us that the 2PI and the exact couplings are the same for the perturbative region, meaning that we can rely on the results obtained by 2PI calculations in this regime. Thus, if we are using couplings that are in the order of the fine structure constant of QED ($\alpha = 1/137$), for instance, one does not even have to worry about the temperature dependence of Eq. (38).

From Eq. (38), it is obvious that the relation depends on the temperature through the fit parameter A_T; this is shown in Fig. 6(a). We can fit the temperature dependence in the form

$$A_T = a(\tanh Tb)^c, \tag{40}$$

where $a = 0.438 \pm 0.002$, $b = 0.123 \pm 0.01$, and $c = 0.17 \pm 0.002$.

Let us consider the zero-temperature limit: $\lim_{T\to 0} A_T = 0$. This tells us that in the zero-temperature limit all α_{ex} corresponding to any α_{2PI} by Eq. (38) vanish. To see this, it is easier to invert the relation and then take the limit, i.e., $\lim_{T\to 0} A_T \ln(\alpha_{\mathrm{2PI}}/A_T + 1) = 0$. This is consistent with the fact that at T = 0 the coupling drops out from the 2PI propagator [4]. More precisely, at $T = 0$ close to the peak,

$$\mathcal{G}_{\mathrm{2PI}}(w) \propto \frac{1}{w}, \quad \text{while } \mathcal{G}_{\mathrm{ex}}(w) \propto \frac{1}{w^{1+\frac{\alpha_{\mathrm{ex}}}{\pi}}}\bigg|_{\alpha_{\mathrm{ex}}=0} = \mathcal{G}_{\mathrm{2PI}}. \tag{41}$$

Therefore, the diverging $\alpha_{\mathrm{2PI}}/\alpha_{\mathrm{ex}}$ relation does not signal a physical singularity; it just means that in order to match the exact theory we have to take into account other diagrams not included in the resummation.

The relation in Eq. (40) is valid up to the dimensionless temperature $T = 12.03$. Above this temperature, the trend of the curves can be seen in Fig. 5(a), namely, that they are more and more shallow for increasing temperature changes. The $\alpha_{\mathrm{2PI}}(\alpha_{\mathrm{ex}})$ curve becomes steeper and steeper, as can be seen in Fig. 5(b). We find for small couplings the expected universal linear relation $\alpha_{\mathrm{2PI}} = \alpha_{\mathrm{ex}} + \ldots$. We can also observe that the $\alpha_{\mathrm{2PI}}(\alpha_{\mathrm{ex}})$ curves diverge at some limiting value of α_{ex}. This can also be seen from the following fit which describes the numerically determined curve quite well:

$$\alpha_{\mathrm{2PI}} = \frac{\alpha_{\mathrm{ex}}}{B_T - C_T\alpha_{\mathrm{ex}}}. \tag{42}$$

The fit parameters can be seen in Table II. This function has a pole at B_T/C_T at each temperature. This is a temperature-dependent quantity; the running of the position of the pole can be seen in Fig. 6(b).

Equation (42) can be interpreted from the point of view of the scale dependence of the coupling constant. For the B-N model, the one-loop running is exact [4] and provides a Landau pole. The value of the coupling for which we find the pole is $\alpha(\mu_0) = \frac{\pi}{\ln \mu/\mu_0}$. If we associate $\mu \sim T$ for high temperatures, this would suggest that the finite-temperature dependence also exhibits a Landau-type pole at $\alpha_{\mathrm{ex}} \sim (\ln fT)^{-1}$. In fact, a two-parameter fit is

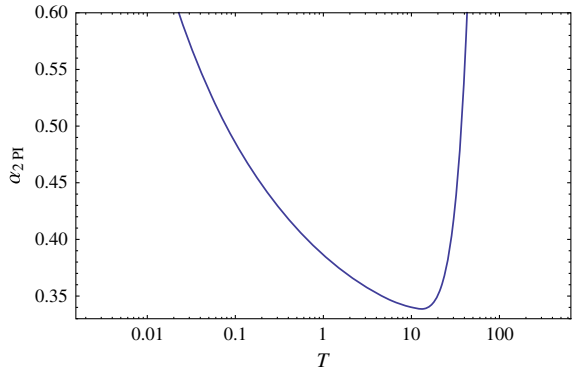

FIG. 7 (color online). Finite-temperature running of α_{2PI} for fixed $\alpha_{\mathrm{ex}} = 0.25$. One can observe the high-temperature (Landau) pole and the $T \to 0$ divergence.

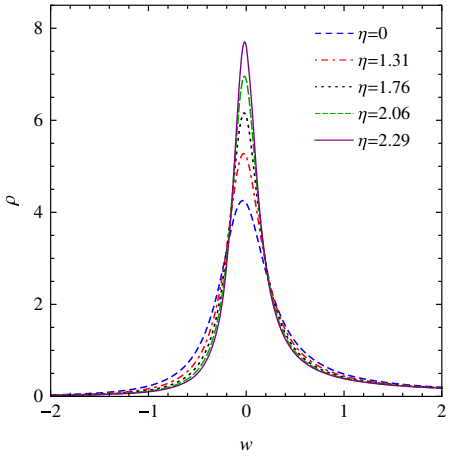

FIG. 8 (color online). The 2PI spectral functions with different rapidities [$\eta = \tanh^{-1}(v)$, where $v = u/u_0$] at fixed temperature $T = 1$ and coupling $\alpha = 0.5$. The shrinking of the width can be observed as the velocity grows, which is the same effect that we had for the exact solution [16].

$$\frac{B_T}{C_T} = \frac{d}{\ln(fT)}, \tag{43}$$

where $d = 0.576 \pm 0.03$ and $f = 0.035 \pm 0.003$ describes the finite temperature behavior for large temperatures.

The finite-temperature running of $\alpha_{2\mathrm{PI}}$ for fixed α_{ex} can be seen in Fig. 7. According to our earlier analysis, we can identify the following characteristic features of this running. For small temperatures, the running of the perturbative coupling is determined by the soft IR physics, the photon cloud. At very small temperatures, seemingly, we find a divergence, but this is not a physical singularity; it just reflects the fact that at zero temperature the 2PI approximation fails to describe the exact spectrum for any couplings, cf. Eq. (41). At high temperatures, the perturbative running is the dominant effect with the association $\mu \sim T$. Again, we find a pole there that comes from the Landau pole of the perturbative running. But, again, this singularity is not a physical one; the exact spectrum is regular for α_{ex} larger than the pole value. But with the 2PI calculation with the original action, we cannot reproduce this result, and one would need to take into account higher point vertices, too. Between the low-temperature and high-temperature regimes, there is a point where $d\alpha_{2\mathrm{PI}}(T)/dT = 0$; in our case, this is at the dimensionless temperature value $T = 12.03$. This is a "fixed point" of the running and loosely determines a "critical temperature" separating the two physically different temperature regimes.

B. Finite-velocity case

We can repeat the same analysis for the finite-velocity case, too. Since the findings are very similar to the $u = 0$ case, we just briefly overview the results.

For the finite-velocity case, we obtained in our previous article [16] the formula in real time,

$$\rho(t) \propto z(t)\rho_{u=0}(t; \alpha_{\mathrm{eff}}), \tag{44}$$

where we defined an effective coupling that incorporates the information about the finite velocity

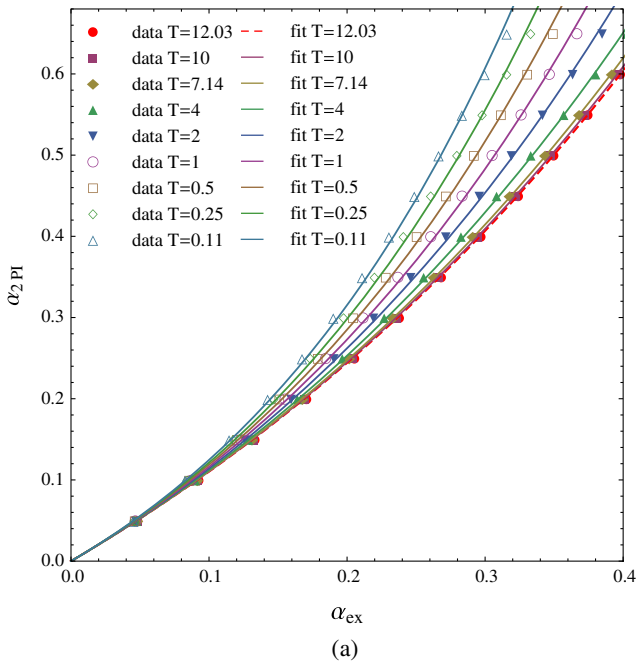

(a)

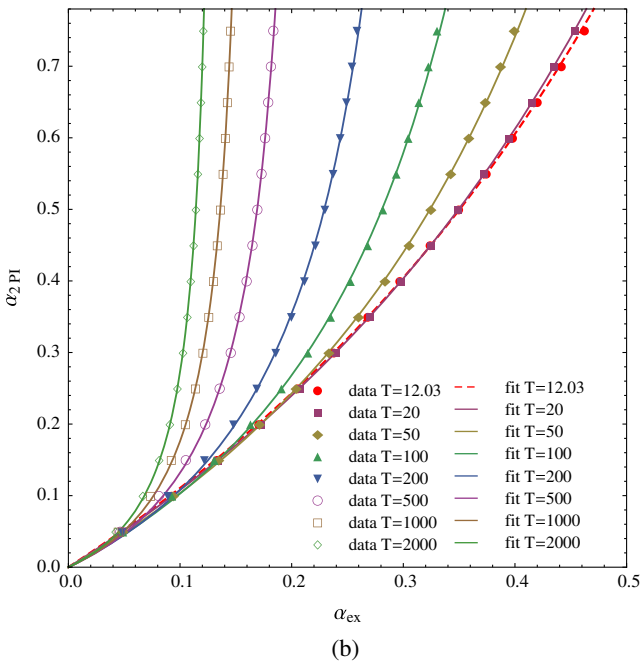

(b)

FIG. 9 (color online). The relation between the 2PI and the exact coupling for $u = \sqrt{3}$ at temperatures (a) $T \in [0, 12.03]$ and (b) $T \in (12.03, \infty)$, respectively. The dashed red line indicates the limiting function at $T = 12.03$; for details, see the text.

TABLE III. The fit parameters in the low-temperature case for $u = \sqrt{3}$.

T	0.11	0.25	0.5	1	2	4	7.14	10	12.03
A_T	0.235 ± 0.002	0.266 ± 0.002	0.298 ± 0.002	0.338 ± 0.002	0.386 ± 0.002	0.442 ± 0.002	0.488 ± 0.002	0.507 ± 0.001	0.517 ± 0.001

TABLE IV. The fit parameters in the high-temperature case for $u = \sqrt{3}$.

T	20	50	100	200	500	1000	2000
B_T	1.016 ± 0.001	1.108 ± 0.007	1.2 ± 0.014	1.29 ± 0.017	1.371 ± 0.0175	1.389 ± 0.0145	1.35 ± 0.009
C_T	0.908 ± 0.002	1.422 ± 0.023	$= 2.275 \pm 0.048$	3.629 ± 0.075	6.113 ± 0.102	8.216 ± 0.105	9.8318 ± 0.079

$$\alpha_{\text{eff}} = \frac{\alpha u_0(1-v^2)}{2v} \ln \frac{1+v}{1-v}, \tag{45}$$

and here $v = \frac{u}{u_0}$. $z(t)$ is a function of time, which is defined as

$$z(t) = \exp\left\{ \frac{u_0(1-v^2)\alpha}{2\pi v} \int_{u_0(1-v)}^{u_0(1+v)} \frac{ds}{s^2} \ln \frac{\sinh \pi t T s}{(\sinh \pi T t)^s} \right\}. \tag{46}$$

In momentum space, the product in Eq. (44) turns into a convolution, and thus one can derive the finite-velocity spectral function only by using numerics. In the 2PI case, we are going to use the same numerical calculation that we had for the $u = 0$ case, and the only difference is that this time we use the formula in Eq. (36) for the discontinuity of the self-energy. The spectral functions obtained from 2PI for different $u > 0$, but fixed temperature and coupling constant, can be seen in Fig. 8.

To fit the $u > 0$ spectral functions, we are applying exactly the same procedure that we used for the $u = 0$ case. For this purpose, we choose the value $u = \sqrt{3}$ (or $v = \sqrt{3}/2$). In Fig. 9, we can find the relation between the 2PI and the exact couplings, and in Tables III and IV, we can find the corresponding fit parameters, but this time for $u = \sqrt{3}$. For the given finite u, we have almost the same picture that we had for the $u = 0$ case, and just the fit parameters, A_T, B_T, and C_T, are different. Interestingly, the threshold temperature stayed at $T = 12.03$, but the running of the parameter as a function of the temperature is slightly modified. Now, we have $A_T = a \tanh(bA_T)^c$, where this time $a = 0.55 \pm 0.01$, $b = 0.075 \pm 0.01$, and $c = 0.183 \pm 0.004$. For the running of the pole, we have $[B_T/C_T = d/\ln(fT)]$ $d = 0.623 \pm 0.04$ and $f = 0.032 \pm 0.003$.

VI. CONCLUSION

We gave a numerical implementation of the 2PI resummation for the fermionic spectral function in the B-N model at nonzero temperature. In our former paper [16], we showed a derivation of the exact spectral function in an analytic way and obtained a closed form. Hence, this analytic formula provides us a good basis point in the benchmarking of the 2PI approximation. The 2PI technique, being an approximation, cannot provide us a full solution, but we can still compare it to the exact result.

Our first main result is that the 2PI approximation works excellently at finite temperatures, and the spectrum coming from the 2PI approximation could be fitted to the exact spectrum with very good accuracy. The two curves could be fitted into each other, not just in the vicinity of the peak but also for much larger momentum interval. This demonstrates that the 2PI resummation is in fact a physically appropriate approximation for gauge theories, too.

Nevertheless, the 2PI and the exact results could be fitted to each other after properly choosing the 2PI coupling $\alpha_{\text{2PI}}(\alpha_{\text{ex}}, T)$ as a function of the coupling of the exact formula (α_{ex}) and the temperature. For a fixed α_{ex}, this describes a temperature-dependent running coupling constant. Our second main result is to provide this function for the B-N model.

This temperature dependence has two distinct regimes for small and large temperatures. At small temperatures, the deep IR physics dominate the running, and the corresponding $\alpha_{\text{2PI}}(T)$ decreases with the temperature. For high temperatures, the finite-temperature running is compatible with the perturbative scale dependence with the choice $\mu \sim T$, and there $\alpha_{\text{2PI}}(T)$ grows with the temperature. At zero temperature and at some (coupling-dependent) high temperatures, we find divergences in $\alpha_{\text{2PI}}(T)$, and in the high-temperature case, it can be associated with the Landau pole. But none of these poles mean physical singularity, just the breakdown of the perturbation theory. Between the two regimes, there is a temperature at which the temperature derivative of $\alpha'_{\text{2PI}}(T) = 0$. The critical temperature of this fixed point is in dimensionless units $T = 12.03$, and this signals the limiting temperature of the soft and perturbative domains.

The success of the 2PI method extended by a nonperturbative running of the coupling constant encourages one to try this strategy also in the cases of other (gauge) theories. The basis of the temperature running could be the matching of a nonperturbatively (e.g., in Monte Carlo simulations) determined physical quantity. Then, using temperature-dependent 2PI couplings, one could perform

other calculations and give predictions for other, numerically hardly accessible physical quantities.

ACKNOWLEDGMENTS

The authors acknowledge useful discussions with M. Horváth, A. Patkós, and Zs. Szép. The project was supported by the Hungarian National Fund Grant No. OTKA-K104292. This research was also supported by the European Union and the State of Hungary, cofinanced by the European Social Fund in the framework of TÁMOP-4.2.4.A/2-11/1-2012-0001 "National Excellence Program."

[1] F. Bloch and A. Nordsieck, Phys. Rev. **52**, 54 (1937).
[2] N. N. Bogoliubov and D. V. Shirkov, *Introduction to the Theories to the Quantized Fields* (Wiley, New York, 1980).
[3] H. M. Fried, *Greens Functions and Ordered Exponentials* (Cambridge University Press, Cambridge, England, 2002).
[4] A. Jakovac and P. Mati, Phys. Rev. D **85**, 085006 (2012).
[5] H. A. Weldon, Phys. Rev. D **44**, 3955 (1991).
[6] J. M. Luttinger and J. C. Ward, Phys. Rev. **118**, 1417 (1960); G. Baym, Phys. Rev. **127**, 1391 (1962); J. M. Cornwall, R. Jackiw, and E. Tomboulis, Phys. Rev. D **10**, 2428 (1974); J. Berges and J. Cox, Phys. Lett. B **517**, 369 (2001).
[7] Yu. B. Ivanov, J. Knoll, and D. N. Voskresensky, Nucl. Phys. **A657**, 413 (1999).
[8] H. van Hees and J. Knoll, Phys. Rev. D **66**, 025028 (2002).
[9] U. Reinosa and J. Serreau, Ann. Phys. (Amsterdam) **325**, 969 (2010).
[10] J. Knoll and D. N. Voskresensky, Ann. Phys. (N.Y.) **249**, 532 (1996).
[11] D. N. Voskresensky, Nucl. Phys. **A744**, 378 (2004).
[12] J.-P. Blaizot and E. Iancu, Phys. Rev. D **55**, 973 (1997).
[13] J.-P. Blaizot and E. Iancu, Phys. Rev. D **56**, 7877 (1997).
[14] H. M. Fried, T. Grandou, and Y.-M. Sheu, Phys. Rev. D **77**, 105027 (2008).
[15] A. I. Alekseev, V. A. Baikov, and E. E. Boos, Teor. Mat. Fiz. **54**, 388 (1983) [Theor. Math. Phys. **54**, 253 (1983)].
[16] A. Jakovac and P. Mati, Phys. Rev. D **87**, 125007 (2013).
[17] N. P. Landsman and C. G. van Weert, Phys. Rep. **145**, 141 (1987); M. Le Bellac, *Thermal Field Theory* (Cambridge University Press, Cambridge, England, 1996).
[18] M. E. Peskin and D. V. Schroeder, *An Introduction to Quantum Field Theory* (Perseus Books Publishing, Reading, MA, 1995).